Forecasting of Solar Photovoltaic System Power Generation using Wavelet Decomposition and Bias-compensated Random Forest

Po-Han Chiang, Siva Prasad Varma Chiluvuri, Sujit Dey, Truong Q. Nguyen
Dept. of Electrical and Computer Engineering, University of California, San Diego
Email: {pochiang, spv, dey, tqn001} @ucsd.edu

***Abstract* — The use of solar photovoltaic (PV) power is a promising solution to reduce grid power consumption and carbon dioxide emissions. However, the benefit of utilizing solar PV power is limited by its highly intermittent and unreliable nature. The non-stationary and non-linear characteristic of solar irradiance makes solar PV difficult to predict by traditional time series and artificial intelligence (AI) approaches. To address the above challenges, we propose a novel technique integrating stationary wavelet transform (SWT) and random forest models. Instead of conventional decompose-and-reconstruct process in SWT, we only apply the wavelet decomposition to extract the information from raw data with better time-frequency resolutions. We also propose a bias-compensation technique to minimize the prediction error. Our experimental results using sensors data from the on-campus microgrid demonstrate the proposed approach is robust to different forecast time horizons and has smaller prediction error.**

***Index Terms*— Renewable energy; Artificial intelligence; Wavelet decomposition; Solar forecast; Random forest, Microgrid**

I. INTRODUCTION

The last few years have seen tremendous growth in the use of solar energy in the residential, commercial, and industrial sectors. According to [1], the cumulative capacity of global solar PV sector reached 178GW in 2014, and it is estimated to reach 540 GW in 2019. A primary challenge for integrating solar power into power grids is the highly intermittent nature of solar irradiance, not only depending on the region and time, but rapid temporal fluctuations, which results in low utilization of solar power or the need of high capacity energy storage due to the mismatch between PV generation and power consumption. Forecasting of solar power is essential not only for efficient management of the power grid but also for better utilization of solar in residential and commercial deployments.

Solar radiation consists of direct and diffuse solar radiation, the latter getting scattered, absorbed, and reflected within the atmosphere, mostly by clouds, but also by particulate matter and gas molecules [2]. The direct and diffuse components together incident on horizontal surface are termed as global horizontal irradiance (GHI), which is converted to electricity by PV panels. The difficulty arises from the fact that PV output power is dependent on geographic location, time, climate and physical characteristics of PV systems. Solar PV forecasting techniques can be classified into three categories based on forecast horizons [3]: intra-hour, intra-day and days ahead forecasting. In this paper, we focus on intra-day forecast (1 to 6 hours ahead) since it provides grid operators timely information to plan the resource accordingly for grid stability.

For the input data used to forecast solar PV, the authors in [4] evaluate forecasting techniques using only historical PV output. The performance is limited since solar irradiance is highly affected by meteorological variables, such as cloud, humidity, and temperature. In [5], cloud images are analyzed to estimate cloud condition and thus predict solar irradiance. However, the forecast is only applicable in very short time period (within 5 minutes) and the technique requires additional image sensors and processing capability of the system. Our goal is to generate intra-day forecasting models for on-site PV systems, so in this paper, we use current PV output and meteorological data acquired from meteorological sensors, such as temperature, humidity and UV index.

Prior work addressing the non-stationary, non-linear characteristic of solar power are classified into four categories [6]: Numerical Weather Prediction (NWP), local sky imagers/sensor arrays, satellite sky imagers and stochastic and artificial intelligence (AI) techniques. The authors in [6] also indicate that the last method performs better for local intra-day forecast. Time Series techniques like Auto Regressive (AR) and AR with eXogenous input (ARX) models have also been applied for Solar PV forecasting [7]. However, the AR and ARX models cannot fully disentangle complex characteristics of the non-stationary solar PV time series and thus lead to weaker forecast performance. The authors in [8] propose the first simple forecasting method using AI and meteorological data to carry out non-linear mapping from input variables to PV output. The performance is not optimized since the choice of input variables and tuning the AI models is absent. In [9], many artificial neural network (ANN) techniques are reviewed for forecasting of solar radiation such as multilayer perceptron (MLP), recurrent neural networks (RNNs) and genetic algorithms, etc. There are two main challenges using ANNs: 1) The black-box nature of ANNs makes it hard to understand the correlation between input variables and predicted PV output and hence improve the prediction performance, 2) the performance largely depends on the setting of parameters of ANN models,

which makes the optimization process opaque and intractable.

One notable issue in forecasting solar PV output is the relation between the forecast horizon and sampling frequency of input data [6]. For example, short term fluctuation (e.g. 5 minutes sampling duration) of the input data may have no effect on 6-hour ahead PV output. Therefore, using raw PV output as a feature does not work well because spurious temporal variations in PV power due to atmospheric changes and cloud cover at the current time instant have no bearing on future PV power output. To obtain better representation and understanding of forecast models, wavelet analysis is applied on the input variables such as temperature data, solar irradiance and PV output. The authors in [10] apply Discrete Wavelet Transform (DWT) to the PV time-series and use ANNs to forecast each component of the wavelet decomposition. Inverse Discrete Wavelet Transform (IDWT) is then employed to reconstruct the predicted wavelet components to compute the prediction of PV output. A major disadvantage of this approach is that if the prediction of one wavelet component is worse than the other wavelet components, the overall forecast performance will be affected due to the wavelet reconstruction process. In [**11**], the authors decompose PV output, temperature, humidity and wind speed into wavelet components, and then manually remove the uncorrelated wavelet components before prediction. However, the criteria and its rationale to choose the wavelet components is absent. The authors in [12] propose a wavelet-coupled support vector machine (SVM) model using daily meteorological variables. The meteorological data used in [12] is accumulated on daily basis, such as daily precipitation and maximum temperature. The benefit of wavelet transform is not utilized due to insufficient temporal resolution and information loss in averaging or accumulating process of input data.

In this paper, we propose a data driven framework to forecast PV output using the current value of PV output and meteorological sensor data. To extract the inherent relationship between all sensors signals, our proposed framework integrates wavelet decomposition and the random forest model, one of the popular machine learning models showing the best PV output forecasting results among eight pervasive regression methods [13]. We also examine the prediction bias and propose an enhanced random forest to compensate the bias. We use data obtained from the microgrid at the University of California, San Diego (UCSD) [14] in our experiments. We show that our proposed technique outperforms other methods in [9, 12]. Moreover, our proposed technique also solves the problem of mismatch between forecast horizons and sampling frequencies by extracting the spectral information from the raw data. Our framework can be extended to other data-driven prediction tasks, which usually deal with disparate sources of information (sensor signals, operating parameters, etc.) generated from complex physical processes.

The rest of the paper is organized as follows. In section II, the theoretical background of wavelet decomposition and random forests is described and the proposed forecast technique is presented. In section III, the performance of the proposed algorithm is evaluated. Finally, we conclude the paper in section IV.

II. THEORETICAL BACKGROUND AND PROPOSED TECHNIQUE

A. Wavelet Decomposition

To extract the true underlying variation in PV power, we use the stationary wavelet transform taking advantage of its multiresolution structure. Though Fourier analysis [15] is a traditional tool for the analysis of global frequencies present in the signal, it lacks temporal resolution when dealing with non-stationary process. Some frequency resolution in Fourier analysis can be exchanged to get better time resolution, which can be performed by defining short duration waves called mother wavelet functions so that the given signal for analysis is projected on this basis function. Wavelet decomposition provides a convenient way for separating the true underlying trend in signals from the spurious short fluctuations [16].

In traditional Fourier transform, the data is projected on sinusoidal basis functions which extend through the span of time domain. The wavelet basis function is parameterized by the translation parameter b and dilation parameter a [16]. Such a basis function is given by,

$$\psi_{a,b}(t) = \frac{1}{\sqrt{a}}\psi\left(\frac{t-b}{a}\right) \tag{1}$$

Equation (1) provides a basis for wavelet transformation. All the input signals to our regression model are decomposed for translation and dilation in order to get a multi-resolution representation. This is the case for continuous wavelet transform. Discrete Wavelet Transform (DWT) basis at dyadic grid level m and time location n is given by [17]

$$\psi_{m,n}(t) = 2^{-\frac{m}{2}}\psi(2^{-m}\cdot t - n), \tag{2}$$

Dyadic grid sampled wavelets are generally orthonormal. Using the basis function in (2), DWT can be expressed as the inner product between the solar PV signal $x(t)$ and the basis function as

$$T_{m,n} = \int_{-\infty}^{\infty} x(t)\,\psi_{m,n}(t)dt, \tag{3}$$

$T_{m,n}$ is the wavelet coefficient at level (or dilation) m and location (or translation) n, and it provides the detail (fine information) presented in the signal.

The scaling function at level m and shift n is associated with signal smoothing and has similar multiresolution form as the wavelet. It is given by

$$\phi_{m,n}(t) = 2^{-\frac{m}{2}}\phi(2^{-m}\cdot t - n), \tag{4}$$

where $\phi_{m,n}$ has the property $\int_{-\infty}^{\infty}\phi_{\mathrm{m,n}}(t)dt = 1$. For orthonormal decomposition, the scaling function is

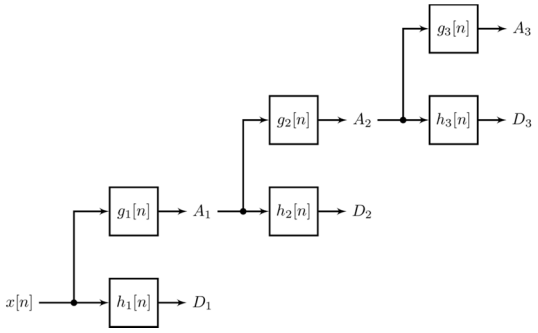

Fig. 1. Digital filter implementation of stationary wavelet transformation.

orthogonal to the translations of itself, but not to its dilations. The smoothing of the signal is obtained by taking inner product of the scaling function with the signal. The obtained samples are called approximation coefficients and are defined as

$$S_{m,n} = \int_{-\infty}^{\infty} x(t)\phi_{m,n}(t)dt, \tag{5}$$

A continuous approximation of the signal can be obtained at level m using the following equation,

$$x_m(t) = \sum_{n=-\infty}^{\infty} S_{m,n}\phi_{m,n}(t), \tag{6}$$

where $x_m(t)$ is a smooth, scaling function-dependent version of the signal at level m. Using approximation coefficients $S_{m_0,n}$ at level m_0 (which can be chosen arbitrarily) and wavelet (detail) coefficients $T_{m,n}$ at levels $1, 2, \cdots, m_0$, the signal can be expressed as follows,

$$x(t) = \sum_{n=-\infty}^{\infty} S_{m_0,n}\phi_{m_0,n}(t) + \sum_{m=1}^{m_0}\sum_{n=-\infty}^{\infty} T_{m,n}\psi_{m,n}(t), \tag{7}$$

There are many wavelet families: Daubechies-4, Daubechies-6, Daubechies-8, Symlet-2, Symlet-4, Symlet-6 etc. In this paper, we use the Symmlet-5 family as its mother wavelet function has similar shape as our solar PV and solar

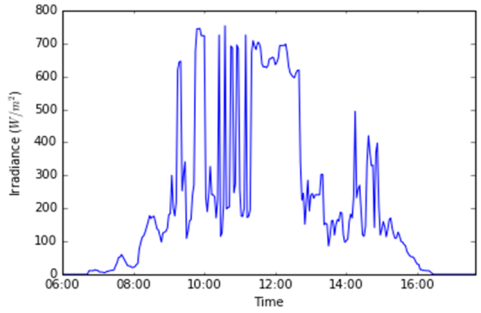

Fig. 2. Solar Irradiance on November 15, 2015.

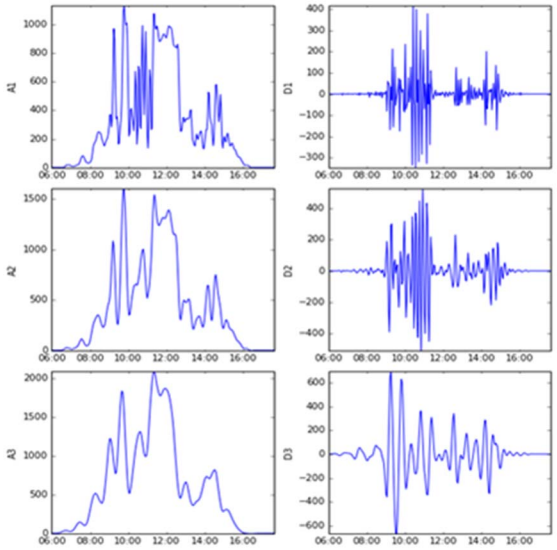

Fig. 3. Wavelet decomposition of solar irradiance on November 15, 2015

irradiance signals and thus allows for efficient analysis of the signal.

We use the stationary wavelet transform which is an extension of the standard discrete wavelet transform that is particularly suited for exploratory statistical and signal analysis [18]. Fig. 1 shows the block diagram of a filter implementation of stationary undecimated wavelet decomposition, where A_1 and D_1 correspond to the approximation and detail coefficients at level 1 respectively. The basic idea behind stationary wavelet transform is to obtain a redundant representation of signal by removing decimation from the discrete wavelet transform. Fig. 2 shows the solar irradiance variation on a typical day (November 15, 2015) and Fig. 3 shows its corresponding stationary wavelet decomposition on the same day where multi-scale variations in solar irradiance are easily noticeable. In Fig. 3, y axis label corresponds to the level and wavelet coefficient type. For instance, A_1 is the level 1 approximation coefficients and D_3 corresponds to level 3 difference coefficients. As the level of decomposition increases, the approximation coefficients become smoother and capture longer duration variations in the signal. For example, in Fig. 3, the level 3 approximation coefficient sequence A_3 is smoother than A_1or A_2 as spurious shorter variations in solar radiation are filtered out in A_3. Similarly, D_1 captures higher frequency (shorter duration) variations than D_2 or D_3. For a given prediction horizon, it is important to choose the right wavelet decomposition level that captures the variation for that time scale. Therefore, there is a need to select the right set of features for the regression model.

B. Random Forests

After applying wavelet decomposition, there may be potentially redundant and irrelevant features. Therefore, the candidate machine learning algorithm should be robust to such kind of features. Here we choose random forests [19], which have been proved to be robust with redundant and

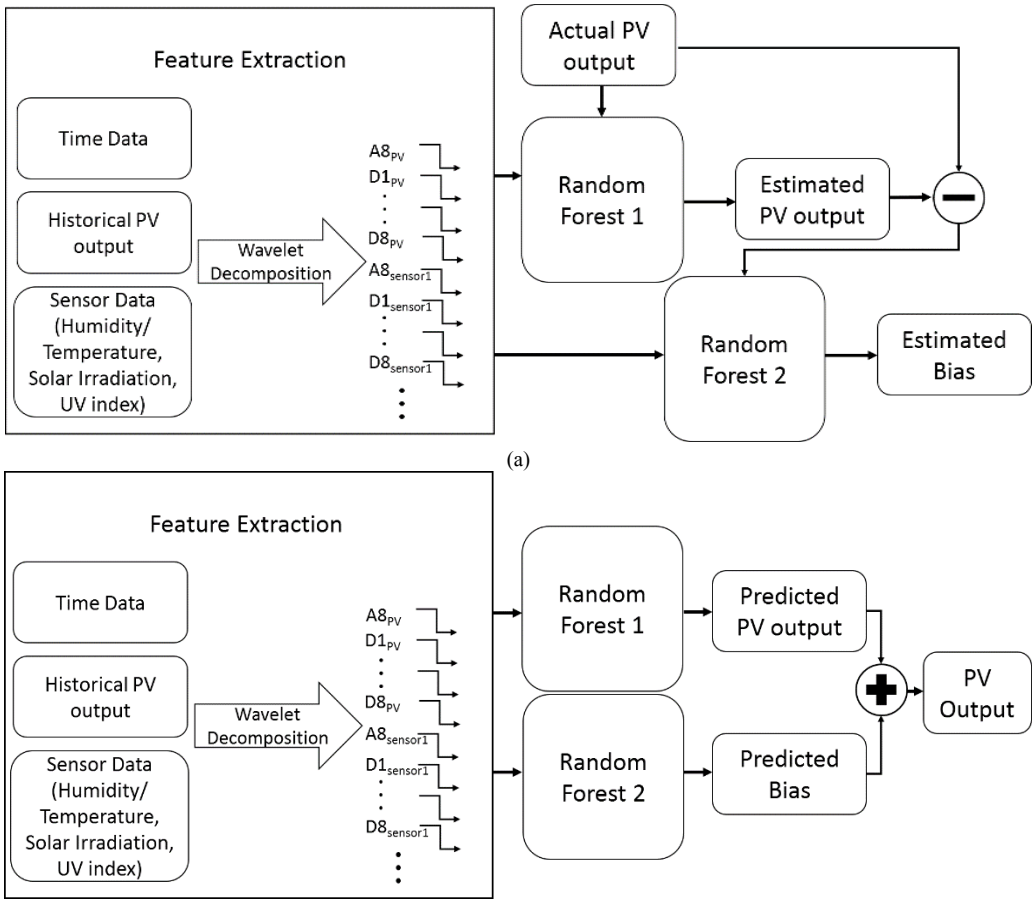

Fig. 4. Block diagram of proposed Wavelet-BCRF (a) upper, training phase (b) lower, prediction phase

irrelevant features [19]. Furthermore, random forests only have two main parameters to be tuned and it is not sensitive to these parameters [20], which facilitates the application of our proposed technique to general solar PV forecast problems.

Preliminaries: decision tree regression:

Decision tree is a non-parametric and tree-like model used in data analytics problems. Decision tree is built by learning simple decision rules inferred from the input data, and each tree consists of three kinds of nodes: 1) root nodes, which represent all the samples that are ready to be split later, 2) decision nodes, which split the samples into multiple sub-trees or leaf nodes based on decision rules, 3) leaf nodes, where no more split is performed. If the target variable is continuous, we call the decision tree a regression tree. At each level of the regression tree, the best feature and its split point are chosen to separate the samples into distinct classes. The choice of the feature and the split point should lead to the greatest reduction in variance for the target variable. The estimated value of the target variable is the mean value of observed samples in that leaf node. In other words, if a new data observation falls into that node, its predicted value of the target variable is the mean value of all samples in that class. Random forest is an enhanced approach of decision trees which usually over-fit the data and result in high variance. The main principle is using a group of weak learners (e.g., decision trees) to form a strong learner. To illustrate random forests, we will first introduce bootstrap aggregation.

Bootstrap samples are datasets randomly drawn with replacement from the training data, and each bootstrap sample is the same size as the original training set. Bootstrap aggregation, or namely bagging, averages the prediction learned from a set of bootstrap samples, thereby reducing its variance [21]. Moreover, since each tree generated in bagging is identically distributed, the expectation of an average of such trees is the same as the expectation of any one of them. Therefore, the bias of bagged trees remains unchanged as that of the individual trees. This leads to a decrease in overall mean squared error, the sum of squared bias and variance. For regression, we train many independent regression trees to bootstrap versions of the training data, and then average the prediction result.

In addition to bagging, random forests further improve the variance by reducing the correlation between the trees, without increasing the variance too much [19]. This is achieved by feature bagging, which randomly selects a subset of input features in each tree-growing process. In summary, a random forest is a collection of uncorrelated decision trees. In practice, random forests generalize well with both

categorical and numerical input features, with minimal parameter tuning required.

C. Proposed Wavelet-BCRF Architecture

Fig. 4 illustrates the architecture of our proposed solar forecast technique with wavelet-coupled feature extraction and bias-compensation random forest (BCRF). First, we conduct stationary wavelet decomposition on all raw input features except timestamps by Symlet-5 wavelet function with eight decomposition layers. The higher level of decomposition includes the lower frequency part of the original signal. We choose a sufficient large number of levels to capture the multi-scale variations of the input signal since random forests are robust with irrelevant features. Therefore, for each input signal x, we can represent it with $A_{x,8}, D_{x,8}, D_{x,7}, \dots D_{x,1}$, To capture the daily periodicity of solar activity, the data is indexed with the sampling interval of sensor data in each day. We then use the wavelet components and time index as input features to train a random forest regression model (termed as Random Forest 1). Note that although feature selection is a common method to enhance the prediction performance, we do not discuss it in this paper. The reason is that the feature bagging method of random forests automatically ranks the importance of features, so it is not necessary to introduce computation complexity or information loss when applying other feature selection methods.

Comparing the predicted PV output and actual PV output, we find that the prediction error is irregularly distributed. For example, there are minimal errors when predicting PV output at night or on sunny days when there is no high frequency fluctuation in the PV output, but more errors on cloudy days when there is high frequency fluctuation in the PV output. Based on this fact, we propose BCRF, which builds an additional model to predict the prediction bias in order to minimize the overall prediction error. As shown in Fig. 4(a), the difference between actual PV output and predicted PV output in the training data is used as the target variable of another random forest model (termed as Random Forest 2) with the same set of input features. In the prediction phase, the predicted PV output and predicted bias, which are generated by two independent random forest models, are summed up as our final prediction, as shown in Fig. 4(b).

III. Application to the Solar PV System in the UCSD Microgrid

A. Data Aquisition

The UCSD microgrid is an advanced microgrid supplying about 85% of the total electricity consumption on the campus [14], with 8% of the total electricity consumption generated by rooftop solar PV. We collect 95 days of data from the UCSD microgrid sensors to test our current solar PV power forecast model. The data set we have is the PV system output on the rooftop of the Supercomputer Center at UCSD and the sensor data from a nearby weather station, which records solar irradiance, UV index, temperature and humidity from indoor/outdoor areas. Our dataset has 55294 records with 2.5 minutes sampling intervals.

Table 1. Comparison of RMSE, MAE, and MAPE of the proposed model with BPNN and W-SVM

	RMSE	MAE	MAPE
BPNN	2.71	1.36	16.01%
W-SVM	1.65	0.89	10.67%
RF	2.22	0.63	7.43%
Wavelet-BCRF	1.12	0.50	5.91%

B. Experiment Results

In this section, we implement and evaluate our Wavelet – BCRF technique using the scikit-learn library in python environment [22] on an Intel i5 3.2GHz quad-cores and 8GB RAM computer. Root mean square error (RMSE), mean absolute error (MAE) and mean absolute percentage error (MAPE) are calculated and used as our evaluation metrics. Their definitions are as follow:

$$RMSE = \sqrt{\frac{\sum_{i=1}^{n}\left(P_{pred}^{i} - P_{actual}^{i}\right)^{2}}{n}}, \tag{8}$$

$$MAE = \frac{\sum_{i=1}^{n}\left|P_{pred}^{i} - P_{actual}^{i}\right|}{n}, \tag{9}$$

$$MAPE = \frac{nMAE}{\sum_{i=1}^{n}\left|P_{actual}^{i}\right|} \times 100\%, \tag{10}$$

We use 5-fold cross-validation to randomly split our data set [14] into training (80%) and test (20%) sets 5 times and average the prediction results. We compare the performance of our proposed approach with multilayer perceptron (MLP) [9], which is one of the most established ANN architectures, Wavelet-coupled SVM (termed as W-SVM) [12] as described in Section I and Random forest without wavelet-transform (termed as RF).

The RMSE, MAE and MAPE of 6 hours ahead forecast of our proposed method and other methods are summarized in Table 1. The error obtained from the BPNN model is among the highest of three methods. The higher forecasting error is possibly because the hidden layer structure does not have the same ability of feature extraction as wavelet decomposition. W-SVM performs better than BPNN, but since W-SVM is originally designed for low sampling frequency (daily basis and 3-level wavelet decomposition), SVM is not as robust as random forests when 8-level wavelet decomposition of data with 2.5 minutes sampling intervals is used. RF performs the closest to Wavelet-BCRF in terms of MAE and MAPE. However, RF falls short on RMSE, which indicates that RF predicts the overall trend of PV output well, but it results in large errors more frequently. Wavelet-BCRF achieves consistently better performance compared with all the three other methods – it reduces by 32.12%, 20.64% and 19.65% in terms of RMSE, MAE and MAPE respectively when compared with the best performance among the other three methods.

Table 2. MAPE in different forecast horizons

	1 hour	3 hours	6 hours
RF	10.31%	8.21%	7.43%
Wavelet-BCRF	6.33%	6.06%	5.91%

Next we will discuss how Wavelet-BCRF stabilizes the prediction performance in different forecast horizons. The MAPE in 1 hour, 3 hours and 6 hours ahead is summarized in Table 2, comparing Wavelet-BCRF with the method using RF. The authors in [6] propose that the sampling period of input data should be chosen depending on the forecast horizon to obtain the best result. However, this may not be possible as the sampling frequency may be determined by other factors such as the sampling rate of the sensors, and different prediction horizons maybe needed for different objectives for the same PV system. As shown in Table 2, using the RF method, the prediction performance for 6-hours ahead is significantly better than the one for 1-hour ahead, which indicates that the 2.5 minutes sampling interval of our data may not originally suit for 1-hour forecast. However, after applying Wavelet-BCRF, we can observe that the prediction performance in different time horizons is much similar (7.11% difference between the highest and lowest MAPE in Wavelet-BCRF compared to 38.76% in RF). The reason is that the wavelet decomposition extracts the information from raw data in different frequencies, and the BCRF can automatically rank the importance of these wavelet components according to different forecast horizons. Therefore, Wavelet-BCRF successfully solves the mismatch between the forecasting horizons and sampling frequencies of input data, and allows the sampling frequency and forecast horizons to be determined independently.

We take the PV output from November 15 to November 17, 2015 as samples to show the difference between predicted and actual PV generation, as shown in Fig. 5. We first examine the case without BCRF. We can observe in Fig. 5(a) that the predicted PV generation (shown in the blue line) correctly tracks the actual PV generation (shown in the black line) except for periods of rapid temporal variations on November 16 and early morning of November 17. We can observe that the prediction error (shown in the red line) is fluctuating and irregularly distributed, so the prediction error cannot be removed by simple models. This fact motivates us to propose BCRF which builds another random forest model to predict and compensate the prediction error.

Fig. 5(b) shows detailed prediction error for November 16 and the comparison between the prediction results with and without BCRF. We can observe that the prediction error is decreased by the proposed BCRF method (shown by the blue line) compared to the case before applying BCRF (shown by the red line). In our experiment, we can achieve an average 6.5% reduction in terms of MAE. The above shows that we further improve the prediction performance of the PV output using BCRF to predict and compensate the bias.

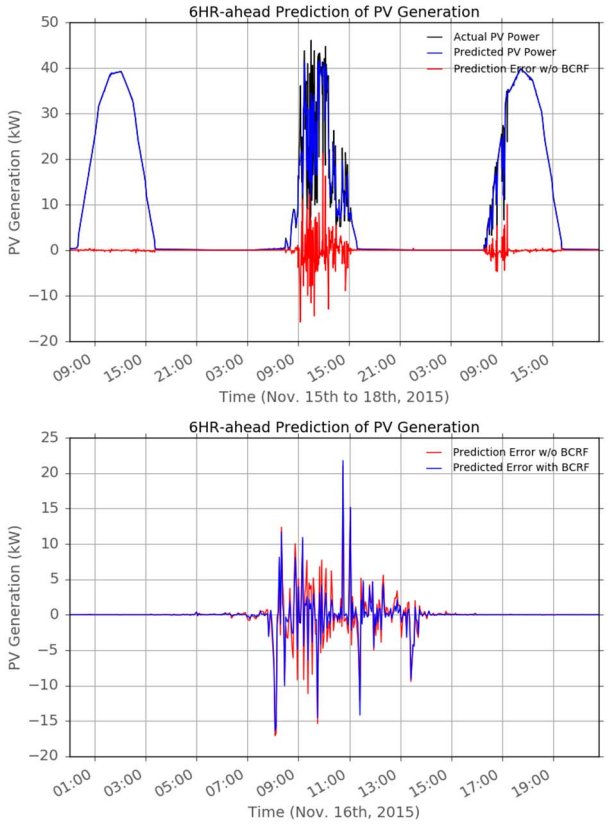

Fig. 5. (a) upper, actual PV power output and 6-hours ahead predicted PV power output on November 15 - 18, 2015 (b) lower, the comparison of the prediction error before and after applying BCRF.

IV. Conclusion

In this paper, we propose a novel solar PV output forecast technique which utilizes stationary wavelet decomposition and machine learning models. By extracting PV output time series and other meteorological variables in increased time and frequency resolution, our technique provides a better representation of the raw data. We also propose a bias compensation technique to enhance traditional random forests by building additional random forest model to estimate the prediction bias. Application to data from the UCSD microgrid PV system shows that our technique can significantly reduce prediction bias compared to conventional approaches and solves the mismatch between the forecasting horizon and sampling period of input data.

V. Acknowledgment

This material is based upon work supported by the National Science Foundation under Grant No. CNS-1619184.

References

[1] Solar Power Europe (SPE)"Global market outlook for solar power 2015-2019" (PDF) URL: www.solarpowereurope.org.
[2] SECO, “Energy Efficiency: Texas' Newest Energy Resource,” 2008.
[3] A. Pavlovski and V. Kostylev “Solar power forecasting performance towards industry standards,” *International Workshop on the Integration of Solar Power into Power Systems*, Aarhus, Denmark, October, 2011.

[4] H. Pedro and C. Coimbra, “Assessment of forecasting techniques for solar power production with no exogenous inputs,” *Solar Energy*, Volume 86, Issue 7, pp. 2017-2028, July 2012.
[5] C. Chow, B. Urquhart, M. Lave, A. Dominguez, J. Kleissl, J. Shields and B. Washom, “Intra-hour forecasting with a total sky imager at the UC San Diego solar energy testbed,” *Solar Energy*, Volume 85, Issue 11, pp. 2881-2893, November 2011.
[6] H. Inman, H. Pedro, and C. Coimbra, “Solar forecasting methods for renewable energy integration,” *Progress in energy and combustion science,* 39.6, pp. 535-576, 2013.
[7] C. Yang and X. Le, “A novel ARX-based multi-scale spatio-temporal solar power forecast model,” *North American Power Symposium (NAPS)*, 2012.
[8] A. Sfetsos and A.H. Coonick, “Univariate and multivariate forecasting of hourly solar radiation with artificial intelligence techniques,” *Solar Energy*, Volume 68, Issue 2, pp. 169-178, February 2000.
[9] A. Yadav and S. Chandel, “Solar radiation prediction using Artificial Neural Network techniques: A review,” *Renewable and Sustainable Energy Reviews*, Volume 33, pp. 772-781, May 2014.
[10] S. Cao and J. Cao, “Forecast of solar irradiance using recurrent neural networks combined with wavelet analysis,” *Applied Thermal Engineering*, 2005.
[11] H. Zhu, X. Li, Q. Sun, L. Nie, J. Yao and G. Zhao, “A Power Prediction Method for Photovoltaic Power Plant Based on Wavelet Decomposition and Artificial Neural Networks,” *Energies,* 9.1: 11 2015.
[12] R. Deo, X. Wen and F. Qi, “A wavelet-coupled support vector machine model for forecasting global incident solar radiation using limited meteorological dataset,” *Applied Energy*, Volume 168, 15, pp. 568-593, April 2016.
[13] M. Zamo, O. Mestre, P. Arbogast and O. Pannekoucke, “A benchmark of statistical regression methods for short-term forecasting of photovoltaic electricity production, part I: Deterministic forecast of hourly production.” *Solar Energy,* 105, pp. 792-803, 2014.
[14] UCSD, “UCSD Microgrid Project,” http://microgridprojects.com.
[15] A. Oppenheim, and R, Schafer, “Discrete-time signal processing,” *Pearson Higher Education*, 2010.
[16] S. Mallat, “A wavelet tour of signal processing,” *Academic Press*, 1999.
[17] G. Strang and N. Truong, “Wavelets and filter banks,” *SIAM*, 1996.
[18] P. Nason, and B, Silverman, “The stationary wavelet transform and some statistical applications.” *Wavelets and statistics,* pp281-299, 1995.
[19] L. Breiman, “Random Forests,” *Machine Learning*, 45(1):5–32, 2001
[20] A. Liaw and M. Wiener, “Classification and regression by random forest,” *R news*, 2(3): pp.18–22, 2002
[21] B. Efron, and R. Tibshirani, “An introduction to the bootstrap,” *CRC press*, 1994.
[22] “scikit-learn Machine Learning in Python,” 2015, http://scikit-learn.org/.